

Excited state properties of sizable molecules in solution: from structure to reactivity

Fabrizio Santoro · Vincenzo Barone ·
Caterina Benzi · Roberto Improta

Received: 27 July 2006 / Accepted: 13 October 2006 / Published online: 5 January 2007
© Springer-Verlag 2006

Abstract We review some recent advances in quantum mechanical methods devised specifically for the study of excited electronic state of large size molecules in solution. The adopted theoretical/computational framework is rooted in the density functional theory (DFT) and its time-dependent extension (TD-DFT) for the characterization of ground and excited states, in the polarizable continuum model (PCM) for the treatment of bulk solvent effects, and in time-dependent quantum mechanical methods for chemical dynamics. Selected applications to the simulation of absorption spectra, to the interpretation of time-resolved experiments, and to the computation of dissociative electron transfer rates are presented and discussed.

Keywords Excited states · Quantum mechanical calculations · Solution · Dynamics · Time-dependent density functional theory

1 Introduction

A deeper understanding of the static and dynamic properties of excited electronic states is fundamental for

many photochemical and photophysical processes of high technological or biological interest [1,2]. Just to make some examples, many advances in the field of laser technology, solar cells, and imaging exploit the possibility of controlling the excited state behavior of suitable photoactive molecules. Electron transfer (ET) reactions, ubiquitous in biological processes such as photosynthesis or oxidative phosphorylation involve excited states, and photoisomerization reactions are at the basis of the vision.

All these fields are receiving significant benefits from the ongoing developments of the experimental techniques allowing for the accurate detection and characterization of short-lived species [3,4]. The continuous progress in the ultrafast laser technology has allowed the developments of new research fields such as femtochemistry, devoted to the understanding and, more recently, to the control of the elementary excited-state reactive chemical processes [5]. Furthermore, the advances in pump and probe time-resolved experiments made absorption and fluorescence spectroscopy, which have always been a source of fundamental information on many chemico-physical molecular features, the ideal tools to monitor the time evolution and the outcome of many reactive processes.

However, due to the large number and complexity of the effects that can potentially influence photophysical and photochemical processes, it is not always easy to disclose all the information contained in the experimental results, limiting the potentialities of these techniques.

In such a scenario, being able to characterize the excited state behavior by using computational techniques would be extremely useful, and it would increase the amount of information derived from experiments [6–8]. Furthermore, theoretical methods make

F. Santoro
Istituto per i Processi Chimico-Fisici, CNR,
Area della Ricerca del CNR Via Moruzzi, 1 56124 Pisa, Italy

V. Barone · C. Benzi · R. Improta
Dipartimento di Chimica, Università Federico II,
Complesso Monte S. Angelo, via Cintia, 80126 Napoli, Italy

R. Improta (✉)
Istituto di Biostrutture e Bioimmagini, CNR,
via Mezzocannone 16, 80134 Napoli, Italy
e-mail: robimp@unina.it

easier to evaluate the mutual influence of the many subtle effects determining the final outcome of a reactive process. This possibility is very important in order to establish some general and transferable rules enabling to predict and, at the occurrence, to alter the dynamics and the fate of the process of interest.

However, using theoretical methods to obtain a static and dynamic description of the electronic excited states in molecules of technological and biological interest is a very demanding task.

First, an accurate quantum mechanical method is necessary to determine excitation energies already in the gas phase. Furthermore, it is important to correctly describe the excited state stationary points, by performing excited state geometry optimizations. Since technological and biological processes usually involve quite large systems, this computational method should be feasible for medium/large size molecules.

Of course, the usefulness of computational methods would be quite limited if environmental effects could not be taken into proper account since almost all the above-mentioned processes occur indeed in solution. As a consequence, even a qualitative agreement with experiments requires the use of a suitable solvation model. The inclusion of environmental effects involves additional difficulties: not only the solvation model should be able to provide an accuracy comparable to that attained in vacuo but also in solution any problem involving excited states becomes intrinsically dynamic. Solvent reaction field couples indeed the ground state density with the density correction and the orbital relaxation arising from the electronic transition. Furthermore, the coupling is modulated by the solvent relaxation times.

The above considerations clearly show that several requirements must be fulfilled in order to obtain a reliable *static* description of the electronic excited states. But chemical processes are dynamical in nature and it is important to pursue also time-dependent approaches to their study. In fact, chemistry is much richer than what stationary states can tell (just think to possible effect of coherence), and this is particularly true in the field of ultrafast processes started or even driven by laser pulses. In the latter situation, stationary states simply do not exist since the molecule is governed by a time-dependent Hamiltonian (see also [9]). Two general schemes are actually pursued to study these processes: classical (CD) and semi-classical (SCD) [10] computations based on the motion of bunches of trajectories released on the excited surface with suitable initial conditions, and proper quantum dynamics (QD) treatment. This latter has a very unfavorable scaling of the computational cost with the dimension of the system to be treated,

even if remarkable improvements have been introduced recently with the MCTDH method [11]. Moreover, QD methods require the knowledge of the functional form of the potential on which the nuclei move. While this is in principle always obtainable by fitting the results of electronic computations on proper grids in coordinate space, this procedure in practice is feasible only for small molecules. CD and SCD methods scale much better with the dimension of the system (especially CD ones) and can be performed “on the fly” computing for each trajectory energy and forces at each propagation step [12]. Unfortunately, CD results in realistic systems may be sensibly different from correct quantum ones [13], and moreover, computational reasons impose to resort to less accurate electronic description when one wants to apply them to large size molecules. Therefore, together with performing all coordinates on the fly CD computations, it is still highly desirable to pursue QD studies on models of restricted dimensionality, based in this case on reliable surfaces obtained with accurate methods. Such studies often reveal of paramount importance to figure out and test possible dynamic mechanisms in ultrafast processes.

In the past few years, considerable effort has been made to deal with excited state problems of even medium size molecules not only in the gas phase [6, 14–17] but also including environmental effects [18–21]. In this paper, we report the basic aspects of our approach, confirming that the recent advances in the quantum mechanical methods allow to reliably treat the excited state behavior of large size molecules in solution. After concisely discussing the most significant aspects of the theoretical/computational framework we employ, we present some selected applications (see Fig. 1).

We will start from the completely *ab initio* calculation of absorption spectra in condensed phase, that, although being one of the most basic experiments involving excited states, requires that many methodological tools have reached a high degree of accuracy. We will then show how the complete exploration of the excited state PES can help in the rationalization of sophisticated pump and probe experiments on interesting molecules such as stilbene, cyanine, and DNA bases.

The discussion of the results concerning the complete *ab initio* calculation of the dissociative electron transfer (DET) rate in polypeptide systems will constitute a further step toward the dynamical characterization of biological systems.

Finally, we will show the potentiality of QD studies on a simple model for the initial mechanism of depletion of the excited population in a derivative of uracil, a DNA base.

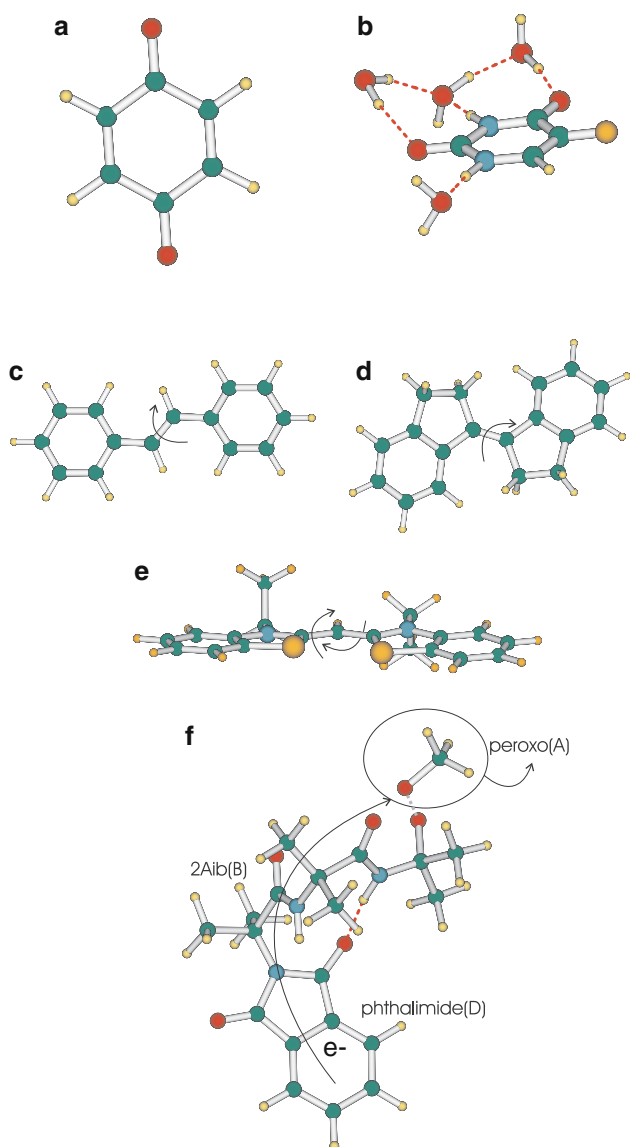


Fig. 1 Schematic picture of the systems and of the processes examined in the present study: **a** Parabenzoquinone; **b** 5fluorouracil-4H₂O; **c,d** *trans*-stilbene and *trans*-stiff stilbene (dihedral rotation involved in the photoisomerization to the *cis* isomers is depicted); **e** NTK88 *trans* (dihedral rotations involved in the photoisomerization to the *cis* and *d-cis* isomers are depicted); **f** Phthalimide-Aib2-peroxo system (DET reaction is depicted)

2 Theoretical methodology

2.1 Excited state calculations

As discussed in the introduction a method coupling accuracy and computational feasibility is necessary. We thus selected the time -dependent extension of density functional theory (TD-DFT) as reference computational method[22–24]. TD-DFT recently emerged as a very effective tool, since, when coupled to suitable

density functionals, it probably represents the best compromise between accuracy and computational cost for describing the excited state behavior in medium/large size molecules, often reaching an accuracy comparable to that of the most sophisticated (but too expensive) post-Hartree–Fock methods[25–30].

The recent implementation of TD-DFT analytical gradients [31–34] allows for the determination of the excited state stationary points and their properties (e.g. the multipole moments), with a good agreement with experiments despite the limited computational costs. Harmonic frequencies can be obtained by performing numerical differentiation of the analytic gradients, and the subsequent vibrational analysis has provided encouraging results in several systems.

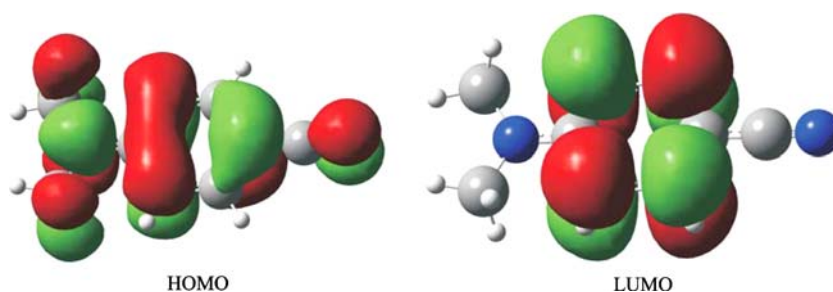
On the other hand, besides the treatment of electronic states within intrinsic multireference character[1, 2], there are other cases in which DFT could exhibit some deficiencies in properly describing excited states (i) involving charge separation, or (ii) with substantial contributions from double excitations [35–38]. In this respect, it is worth noting that interesting attempts to overcome the above limitations have been recently proposed [37–43]. However, for electronic transitions which involve only partial intramolecular charge transfer(CT), the underestimate of the excitation energies by TD-DFT, due to spurious self-interaction, may be controlled by the use of hybrid functionals. An example is provided by 4-(*N,N*-dimethylamino)benzonitrile, where the molecular orbitals involved in the CT transition partially overlap (see Fig. 2).

Gas-phase test calculations [44] performed using the PBE0 functional [45] and various basis sets provide overestimates equal to $\Delta E = 0.29$ eV (6-31G(*d*) basis set), $\Delta E = 0.16$ eV (6-311+G(*d,p*)) and $\Delta E = 0.14$ eV (aug-cc-pVDZ) over the experimental value 4.56 ± 0.1 eV [46]. Previous TD-DFT calculations [47] using B3LYP functional and TZVPP basis set provided $\Delta E = 0.11$ eV. All TD-DFT results are comparable to excitation energies computed using post-HF methods, such as multireference perturbation configuration interaction (CIPSI, $\Delta E = 0.22$ eV [48]), CASPT2/ANO (DZ) [49] ($\Delta E = -0.18$ eV) and STEOM-CCSD/cc-pVTZ [50] ($\Delta E = 0.14$ eV).

Moreover, if a full investigation of the PES coupled with a higher degree of accuracy is needed, the most efficient approach is an integrated protocol using TD-DFT to explore wide regions of the PES and a more sophisticated computational method to refine the energetic of the reaction.

As already pointed out, the accuracy of the computational results depends on the density functional employed. We choose PBE0 hybrid functional [45], in

Fig. 2 Molecular orbitals involved in the CT transition for 4-(*N,N*-dimethylamino)benzonitrile



which the spurious self-interaction is partly cured by hybridization with Hartree–Fock exchange. In PBE0 the amount of exact exchange has been determined in order to fulfill a number of physical conditions, without resorting to any fitting procedure [45]. PBE0, obeying both the Levy condition [51] and the Lieb-Oxford bound [52], provides a fairly accurate description of the low density/high-gradient regions. On the average, TD-PBE0 excitations energies are thus more accurate than those provided by other commonly used hybrid functionals, such as B3LYP [25]. Despite the absence of adjustable parameters, PBE0 has thus shown to provide a reliable description of the conformational equilibria [53–56] and the excited state in biological systems [25–29], as well as an overall degree of accuracy comparable with that of the best last generation functionals [57].

Density functional theory has shown to be able to provide a reliable prediction of the vibrational frequencies and using TD-DFT is possible to obtain a balanced description of the ground state and excited state vibrations.

2.2 Solvation model

On the ground of our previous experience, we selected the so-called polarizable continuum model (PCM) [58, 59] as a reference method for including solvent effect. In this model the solvent, represented by an homogeneous dielectric, is polarized by the solute, placed within a cavity built as the envelope of spheres centered on the solute atoms. The solute–solvent electrostatic interaction operator is defined in terms of a set of apparent surface charges placed in the middle of the tesserae, i.e. the small tiles which the cavity surface is finely subdivided in.

Polarizable continuum model has shown to provide a reliable description of solvent effects on both ground and excited state properties [58, 59]. A PCM formulation directly applicable to TD-DFT calculations does exist [60], and it has been successfully applied to the study of the spectroscopic behavior of the several chemical systems in solution. Furthermore, analytical first derivatives have been recently implemented, allowing

for effective excited state geometry optimizations [34]. Finally, besides the traditional implementation based on linear response theory [60], a new state-specific version of PCM/TD-DFT (allowing for a more balanced treatment of dark and bright electronic transitions) has been recently proposed [61].

When dealing with excited states properties in solution, it is important to take solvent relaxation time into the proper account. A simple but very used approach is to define two limit regimes for the solvent degrees of freedom: the non-equilibrium and the equilibrium regime [62, 63]. The former is more suitable for treating solvent reaction field to very sudden variations of the solute electronic density (as those involved in an electronic transition). In this regime, only solvent electronic polarization is in equilibrium with the excited state electron density of the solute, while the solvent nuclear polarization remains equilibrated with the ground state electron density. The equilibrium regime corresponds to processes “slow” enough (for example emission from long-lived excited states) to allow the whole solvent nuclear relaxation. In this case, all the solvent degrees of freedom are in equilibrium with the electron density of the state of interest.

Both equilibrium and non-equilibrium effects can be easily treated within the framework of the PCM method. The solvent reaction field in the non-equilibrium regime depends in the PCM formalism on the dielectric constant at optical frequency (ϵ_{opt} , usually related to the square of the solvent refractive index n , $\epsilon_{\text{opt}} = n^2$). PCM equilibrium solvation is instead ruled by the static dielectric constant (ϵ). More complex time dependent solvation effects can also be described in the PCM framework, simply by introducing a time dependence in the apparent charges [64, 65].

Finally, it is worth of mention that in several systems bulk solvent effect is not sufficient for an accurate treatment of the statistical and dynamical of the excited state properties. In those cases, the inclusion of a limited number of explicit solvent molecules of the cybotactic region is usually able to restore the agreement between computation and experiments [66, 67].

2.3 Time-independent approach to the computation of CW spectra

Optical continuous-wave (CW) spectra measure the intensities of radiative transitions between molecular stationary states. It is thus possible to compute them relying entirely on a time-independent approach (an alternative route is possible, see Sect. 2.4). We focus here on absorption spectra but the computation of fluorescence spectra is completely analogous. The energy-domain expression for the stick absorption spectrum from the electronic state $|e'\rangle$ to $|e\rangle$ is

$$\sigma_{abs}(\omega) = \frac{4\pi^2\omega}{3c} \sum_{j'j} p_{j'} |\mu_{j'j}|^2 \delta(E_{j'} - E_j + \hbar\omega), \quad (1)$$

where $\mu_{j'j} = \langle j' | \langle e' | \mu | e \rangle | j \rangle$ are the transition dipole moments, $|j'\rangle$ and $|j\rangle$ the vibrational states of $|e'\rangle$ to $|e\rangle$, respectively, $E_{j'}$ and E_j their energies and $p_{j'}$ the Boltzmann population of initial states $|j'\rangle$ [68]. In condensed phase finite-time relaxation of the solvent can indeed affect the spectrum by modulating the energies and wavefunctions of the vibrational states $|j\rangle$. Therefore, it is useful to adopt the approach of the two time-regime limits described in the previous section, and define consequently non-equilibrium (σ_{abs}^{neq}) equilibrium (σ_{abs}^{eq}) limits to the spectrum [62]. In line of principle the non-equilibrium limit is more suited for absorption spectra. Nonetheless, when dealing with fluorescence spectra the ability to describe equilibrium/non equilibrium regimes [62] and possible intermediate cases can make calculation of spectra a powerful though an indirect tool to investigate solvation dynamics for large systems. We have developed a general computational method to compute absorption spectra for medium/large size molecules, which is grounded in the framework of the harmonic approximation. State-of-the-art TD-DFT calculations [69] allow a complete and balanced description of the molecular vibrations of ground and excited electronic states for medium/large size molecules, also in condensed phase when coupled to the PCM method. Transition moments (see Eq. 1) can therefore be computed if one is able to evaluate Franck–Condon (FC) overlaps among generic vibrational states of the involved electronic states. This is done exactly according to the recursion formula of ref [70]. However, a judicious choice of the integrals to be computed is mandatory when dealing with medium-size molecules (N vibrational modes) if one wants to avoid unfeasible computational costs (considering up to quantum number m on each oscillator requires the computation of a number m^N integrals. Such a number grows steeply with N , becoming easily unaffordable).

We devised an efficient selection criterium which is based on intensity, and an a priori estimate of the values of the set of integrals to be computed [71, 72], and implemented it in a development version of the Gaussian package [73].

2.4 Time-dependent methods for chemical dynamics

Besides being mandatory in the description of dynamical processes, time-dependent methods also provide alternative routes to compute static quantities as in the case of CW absorption spectra, according to the expression [68]

$$\sigma_{abs}(\omega) = \frac{4\pi\omega}{3\hbar c} \sum_{j'} p_{j'} \Re \left[\int_0^\infty dt \langle e' | \langle j' | \mu U_M(t) \mu | j' \rangle | e' \rangle \exp(i(E_{j'} + \hbar\omega)t/\hbar) \right], \quad (2)$$

where $U_M(t)$ is the evolution operator depending on the molecular Hamiltonian H_M , and \Re indicates that only the real part of integral must be considered.

Our computational methodology is well suited for model systems of ultrafast (also non-adiabatic) chemical processes in reduced dimensionality which can be faced by a full quantum-dynamical treatment. Nuclear wavefunction is expressed on the set of basis functions (FBR, function basis representation) or on a grid of points (Fourier method) and it is propagated in time by numerically solving the time-dependent Schrödinger equation [74]. This is accomplished utilizing different propagators, and in particular the re-orthogonalized Lanczos [75, 76] one. This scheme also allows, with only a modest increase of the computational cost, to take into explicit account the action of time-dependent electromagnetic fields.

In the aim to develop general tools for quantum dynamics, the representation of the nuclear wavefunction on a grid of points is very promising since, making diagonal the potential operator, it allows to solve automatically the problem of the computation of potential integrals (which becomes a sum over the grid), providing a general method applicable to each particular case without the need to adequate the integration scheme to the chosen basis sets and to the functional form of the potential.

3 Some case studies

3.1 Simulation of absorption spectra

The integration of some of the methodological procedures described above allows to compute fully ab initio

the absorption spectrum of large molecules in solution, without introducing any parameter, apart inhomogeneous broadening. When dealing with the very demanding case of coumarin 153 in two solvents of different polarity (cyclohexane and dimethylsulphoxide), the computed absorption spectra are in very good agreement with the experimental ones [71, 72]. The 0–0 transition energies computed in the gas phase by PBE0/6-31G(d) and TD-PBE0/6-31G(d) calculations are extremely close to their experimental counterparts. The discrepancy between our computations and the experiments is only $\approx 200 \text{ cm}^{-1}$, confirming the reliability of the vertical excitation energies and of the vibrational frequencies provided by the TD-PBE0 method. The presence in the cyclohexane spectra of two strong features with a comparable intensity spaced by $\approx 1,300 \text{ cm}^{-1}$ is reproduced by our PCM/TD-PBE0 computations. Finally, the computed cyclohexane \rightarrow dimethylsulphoxide solvent shift is underestimated by just $\approx 300 \text{ cm}^{-1}$ with respect to the result derived by the analysis of the experimental spectra. Those results show that solvent effects on the absorption spectra are reliably treated by PCM/TD-DFT calculations.

As a further application of our methodological procedure, we present the computed spectra of parabenzoquinone in the gas phase and in DMSO.

In Fig. 3 we report the stick absorption spectrum, computed in the Condon approximation (transition dipole moments independent of the nuclear coordinates) both in gas phase and in DMSO solution, for the $S_0 \rightarrow S_4$ transition. It is a $\pi-\pi^*$ transition where the π^* orbital has mainly an antibonding character on the C–O bonds. Possible non-adiabatic couplings have been neglected. We performed geometry optimizations and frequency analysis, for both the ground and excited states adopting the DFT and TD-DFT method respectively, the PBE0 hybrid functional and the standard 6-31G(d) basis set. Solvent has been described by the PCM method. The spectrum has been computed for a thermal ($T = 300\text{K}$) distribution of the initial states but when convoluted with a Gaussian with HWHM = 0.01 eV it coincides with the $T = 0\text{K}$ spectrum, which we use for assignment of the main bands. The DMSO spectrum is also convoluted with a broader Gaussian (HWHM = 0.1 eV) to take into account the effect of solvent fluctuations. Three main overlapping progressions can be individuated that involve oscillators m_6 (a squeezing of the ring along the direction of the two C–O bonds), m_{18} (a symmetric bending of the four hydrogen atoms) and m_{26} (a symmetric stretching of the two C–O bonds and the two parallel C–C ring bonds). The solvent modifies the spectrum both shifting the band maximum and altering its shape. We predict a solvent red shift of $\approx 0.18 \text{ eV}$

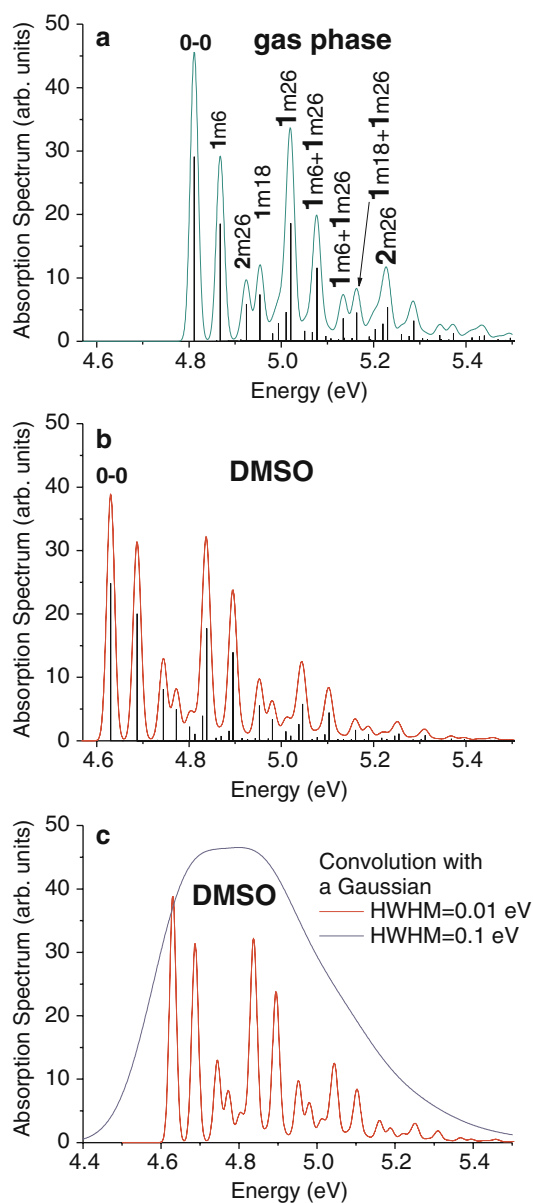


Fig. 3 Computed absorption spectrum $S_0 \rightarrow S_4$ of parabenzoquinone. **a** Stick spectrum in gas phase and its convolution with a Gaussian with HWHM = 0.01 eV with the assignment of the main bands (normal modes are named mX in the order of increasing frequency, where X is the order number); **b** stick spectrum in DMSO convoluted with the same Gaussian as in **a** (the assignment of the main bands coincides with the gas phase case); **c** spectrum in DMSO convoluted with two different Gaussians

(measured from the position of the 0–0 bands). Concerning the spectrum shape, the progressions along the m_6 and m_{26} modes are enhanced in DMSO with respect to gas phase. This feature can be traced back to the fact that the shift in the equilibrium position of these two modes is larger in DMSO than in gas phase due to the combined effect of the electronic character of the tran-

sition and the solvent polarity. As a consequence, the intensity of the band with 1 quantum on the m_{26} mode is 0.74 in gas phase and 0.83 in DMSO, and the order of the intensities of the bands with 1 quantum on m_{18} and 2 quanta on m_6 is reversed.

3.2 Interpreting ultrafast time-resolved experiments

In this section, we present some selected examples of the usefulness of a complete characterization of the excited state PES in order to interpret the results of femto-second pump and probe experiments on molecules of high biological and technological interests, namely, uracil derivatives, stilbene derivatives and cyanines (see Scheme 1).

Fluorescence upconversion experiments on uracil derivatives have shown that the excited-state lifetimes are dominated by an ultrafast (<100 fs) component, with the exception of 5-substituted compounds, exhibiting longer excited-state lifetimes. In analogy with the results concerning other nucleobases [77–82], our calculations indicate indeed that the key motion for the excited state decay is the pyramidalization and out-of-plane motion of the substituents on the C5 atom. A thorough analysis of the excited-state potential energy surfaces, performed at the PCM/TD-DFT(PBE0) level, shows that the energy barrier separating the local minimum on the excited state surface from the conical intersection increases going from uracil through thymine to 5-fluorouracil, in line with the experimental lifetimes [67].

Another interesting result interpreted with the help of PCM/TD-DFT computations concerns solvent effect on excited state lifetimes of 5-fluorouracil [83]. Experiments show indeed that when going from water to acetonitrile solution the fluorescence decay of 5FU becomes three/four times faster. As shown in Fig. 4, computations suggest that this result is related to the opening of an additional decay channel in acetonitrile solution due to the crossing of the bright $S\pi$ (π/π^*) state with an underlying dark Sn (n/π^*) excited state. This channel is closed in water, since the Sn state lies at higher energies (see [84]).

When applied to stilbene and stilbene derivatives (the so-called stiff stilbenes), our computational analysis indicates that the photoisomerization process before barrier crossing occurs on the HOMO \rightarrow LUMO bright state (B_{HL}) [85]. Contrary to previous suggestions based on CASPT2 results (see Fig. 5) [86], the role played by other single-excitation states appears instead negligible. The second state $B-$ is erroneously the lower one at the CASPT2 level, and is close to B_{HL} at MS-CASPT2 level [86]. At the TD-PBE0 level $B-$ is ≈ 0.6 eV above

B_{HL} , as it happens for stiff stilbene (stiff2) in agreement with experimental results [87]. The relative energy barriers on the isomerization paths are consistent with the experimental excited-state lifetimes, supporting the reliability of our results.

A thorough inspection of the ground and the excited states of cyanine NK88 [88] allowed to get significant insights on its short-time ($\approx 1/10$ ps) [89] and long-time ($\approx 10/1,000$ ps) photophysical behavior [90]. The existence of three possible isomers for this cyanine (*trans*, *cis*, *d-cis*), indicated by our PBE0/6-31G(d) results, is the most straightforward way to explain bi-exponential decay of the 400 and 460 nm signals, as due to the thermal coupled back-reactions $d-cis \rightarrow cis \rightarrow trans$ on the S_0 surface.

The short-time dynamics are also governed by two timescales: a shorter one, decaying with less than 2 ps and a longer one with about 9 ps. Inspection of the excited state surfaces suggests that this feature is related to the existence of two competing paths differing in the molecular twisting on the excited surface after photoexcitation.

3.3 Determining ET and DET rate constants

Marcus equation 3 represents a cornerstone for the calculation of the rate constants for thermal ET and DET involving weakly coupled donor (D) and acceptor (A) sites [91].

$$k_{ET} = \frac{2\pi}{\hbar} \frac{H_{DA}^2}{\sqrt{4\pi\lambda k_B T}} \left[\exp\left(-\frac{\Delta G^\ddagger}{k_B T}\right) \right] \quad (3)$$

The reorganization free energy λ is usually computed by considering the energy of the product state when the intramolecular and the solvent degrees of freedom are those of the reactant state minimum.

The well-known Marcus equation is usually employed to compute the activation free energy ΔG^\ddagger :

$$\Delta G^\ddagger = \frac{(\Delta G^0 + \lambda)^2}{4\lambda}, \quad (4)$$

where ΔG^0 is the free-energy difference between the reactants

Finally, the most used model for determining H_{DA} (the D/A electronic coupling H_{DA}) is probably the Mulliken–Hush model, whose key relationship is [94]:

$$H_{DA} = \frac{\mu_{12}^a \Delta E_{12}^a}{\Delta \mu_{DA}^d}, \quad (5)$$

Fig. 4 Computed PES of the $S\pi$ S_n states connecting the FC and the minimum of $S\pi$ for 5fluorouracil in acetonitrile and 5fluorouracil·4H₂O in water solution. The 3N-6 coordinates are grouped in “in-plane” and “out-of-plane” degrees of freedom, with substantial contribution of the C5–C6 bond stretching and C2–N3–C4–C5 dihedral torsion, respectively

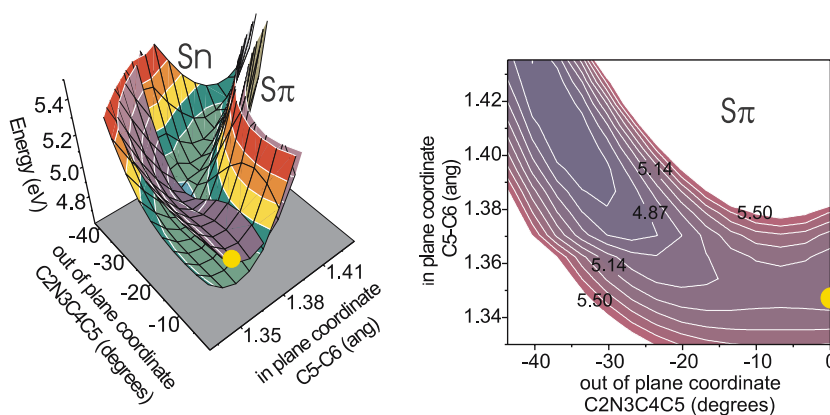
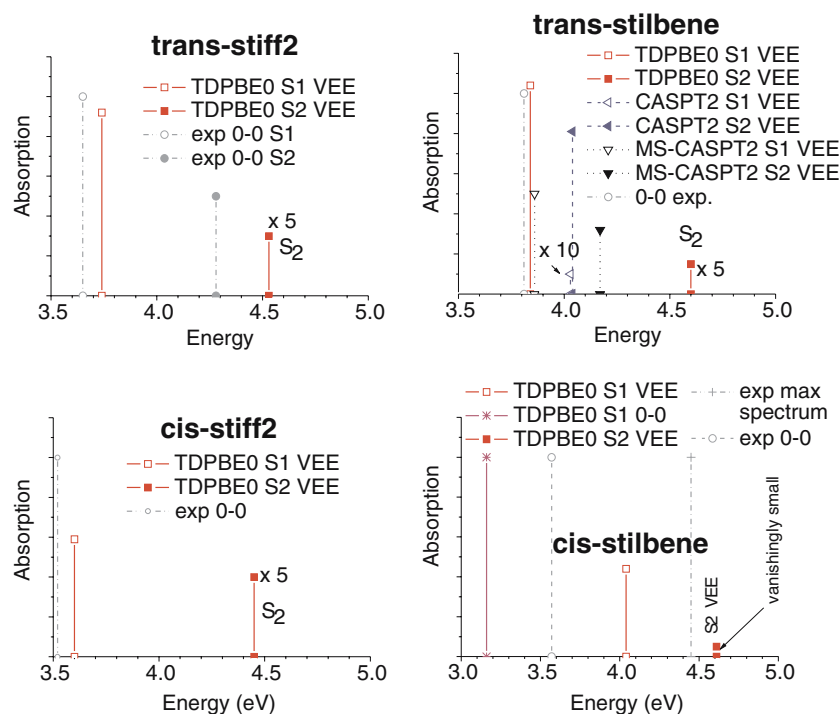


Fig. 5 Vertical excitation energies (VEE) for the *cis* and *trans* isomers of stilbene and stiff stilbene. The 0–0 experimental bands are also reported and compared, for *cis*-stilbene, with the computed adiabatic energy difference (AED). For *trans*-stilbene the TD-PBE0 VEE are compared with those obtained at CASPT2 and MS-CASPT2 level [86]



where $\Delta\mu_{DA}^d$ corresponds to the dipole moment shift

$$\Delta\mu_{DA}^d = \left[(\Delta\mu_{12}^a)^2 + 4(\mu_{12}^a)^2 \right]^{\frac{1}{2}} \quad (6)$$

whereas ΔE_{12}^a and μ_{12}^a are the adiabatic vertical transition energy and the transition dipole moment. In the case of thermal ET, at the transition state, Eq. 5 reduces to

$$H_{DA} = \frac{\Delta E_{12}^a}{2}. \quad (7)$$

It is thus clear that the knowledge of excited state properties [95–98] is very important for computing the key factors determining the ET rate. In two recent papers,

we have shown that all the ingredients necessary to compute ET and DET rates in solution from first principle calculations are nowadays available [99, 100].

We have applied our integrated PCM/PBE0/PCM/TD-PBE0 computational procedure to the study of a donor–bridge–acceptor system, where a phthalimide and a peroxy moiety acts as donor and acceptor, respectively, while the bridge is composed by α amino-isobutyric acid (Aib) peptide units. The computed values for ΔG^\ddagger , H_{DA} , and λ are in good agreement with the estimates obtained by experiments. For the compound containing one peptide unit, the computed ($\log k_{ET} = 4.20$) and the experimental ($\log k_{ET} = 4.70$) DET rates are remarkably close. Furthermore, our calculations predict that when one Aib unit is added to the bridge, the DET rate drops by 3.5 ~ 4.1 log units, in nice agreement with

the experimental results (4.5 log units)[99,100]. Those results seem to indicate that it is now possible to reliably compute of ET and DET rates in large size systems without using any “ad hoc” empirical parameter.

3.4 Unveiling dynamical features

Exact quantum dynamics on restricted-dimensionality potential surfaces derived from accurate electronic calculations can be very important in unveiling the mechanism of ultrafast chemical processes. As an example, a study on a 2D model for the photoisomerization of the protonated Schiff basis of the retinal [101] chromophore has provided a plausible explanation for the bi-exponential depletion of its excited S_1 population [13]. Here we show some results on an idealized 2D model for the $S\pi/Sn$ interaction effect on the depletion of the $S\pi$ excited population of 5fluorouracil (see Fig. 1) in acetonitrile.

Figure. 4 indicates that just after the excitation on the $S\pi$ state, there is a very scarce driving force to removing the planar configuration (actually notice that at the FC point, indicated by the yellow spot, the $S\pi$ surface is bound along the out-of-plane coordinate, though very slightly). Further exploration of the PES along planar coordinates [84] confirms that the initial motion preserves the planarity and can be described by a single collective coordinate r , mainly coinciding with the C_5C_6 bond stretching (notice that r is partially different from the in-plane coordinate in Fig. 4 inasmuch r leads to a planar stationary point on $S\pi$ while the coordinate in Fig. 4 leads to its the non-planar absolute minimum). On the other side, qualitative arguments indicate that $S\pi$ and Sn states do not interact at planar configurations [102] and that the coupling among these diabatic surfaces must depend on a non-planar coordinate [77]. On the ground of these considerations a basic model for the initial dynamics after FC preparation on $S\pi$ can be restricted in two coordinates r and ϕ . Here we show some preliminary results on the following idealized model:

$$H(r, \phi) = H\pi(r, \phi)|S\pi\rangle\langle S\pi| + Hn(r, \phi)|Sn\rangle\langle Sn| + Hn\pi(r, \phi)(|Sn\rangle\langle S\pi| + \text{c.c.}) \quad (8)$$

$$Hn(r, \phi) = \frac{1}{2}m_r\omega_r^2(r - r_n)^2 + \frac{1}{2}m_\phi\omega_\phi^2\phi^2 \quad (9)$$

$$H\pi(r, \phi) = \frac{1}{2}m_r\omega_r^2(r - r_\pi)^2 + \frac{V_2(\phi) + V_4(\phi)S(r)}{1 + S(r)} \quad (10)$$

$$V_2(\phi) = \frac{1}{2}m_\phi\omega_\phi^2\phi^2 \quad (11)$$

$$V_4(\phi) = \frac{1}{2}m_\phi(\omega_{2\phi}^2\phi^2 + \omega_{4\phi}^2\phi^4) \quad (12)$$

$$Hn\pi(\phi) = C\phi \exp(-\phi^2). \quad (13)$$

The $H\pi$ profile along ϕ changes as a function of r (through the switching function $S(r) = \exp[ar^2]$) from a parabola V_2 in the FC region to a double-well V_4 in the proximity of the stationary point on $S\pi$. This feature is introduced as a limit case of the situation in the real molecule where according to our calculations the path to distort the planarity is practically closed at FC (see Fig. 4) while it opens after a planar motion along r [84]. Hn is simply a 2D paraboloid, whose minimum is located at zero along the non-planar coordinate ϕ . This is in partial disagreement with respect to Fig. 4 (where Sn has a minimum at $\phi \approx 20^\circ$) and represents a limit case where the population transfer $S\pi \rightarrow Sn$ is more difficult than what it should be in the real molecule. The coupling $Hn\pi$ depends on the non-planar coordinate ϕ and has the simplest functional form with the right symmetry (linear at the crossing point) and then is damped at large ϕ values to avoid non-physical strong coupling away from it. We work in mass-weighted coordinates and the parameters of the model are determined so to approximately fit our TDDFT results of [84] ($\omega_r=1,600 \text{ cm}^{-1}$, $\omega_\phi = 300 \text{ cm}^{-1}$, H_p frequency along ϕ in the absolute minimum 420 cm^{-1} , $r_\pi=1.43 \text{ \AA}$, $r_n=1.38 \text{ \AA}$, $r_{FC} = 1.346 \text{ \AA}$). The two resulting adiabatic surfaces S_1 and S_2 , respectively, are shown in Fig. 6. The system is prepared at time $t = 0$ by an instantaneous FC excitation $S_0 \rightarrow S\pi$ and Fig. 6 reports the time-dependent population in the state Sn as a function of the coupling factor C in Eq. 8.

It can be seen that already moderate couplings move some population in the dark Sn state, even in the present over-simplified model where (i) the region of the interaction between $S\pi$ and Sn is more limited than that in the real molecule (because the energy gap at $\phi \neq 0^\circ$ between H_n and H_p is larger than the one in the real molecule between Sn and $S\pi$) and (ii) Sn has no channel to drive away the population from the crossing region (as it could be an Sn/S_0 conical intersection). On the contrary, no $S\pi \rightarrow Sn$ population transfer is possible in water where the two $S\pi$ and Sn surfaces do not cross. These results are in line with the fact that the $S\pi$ fluorescence decays more slowly in water than in acetonitrile.

4 Concluding remarks

In this paper, we have summarized the main features of our methodological approach to the characterization

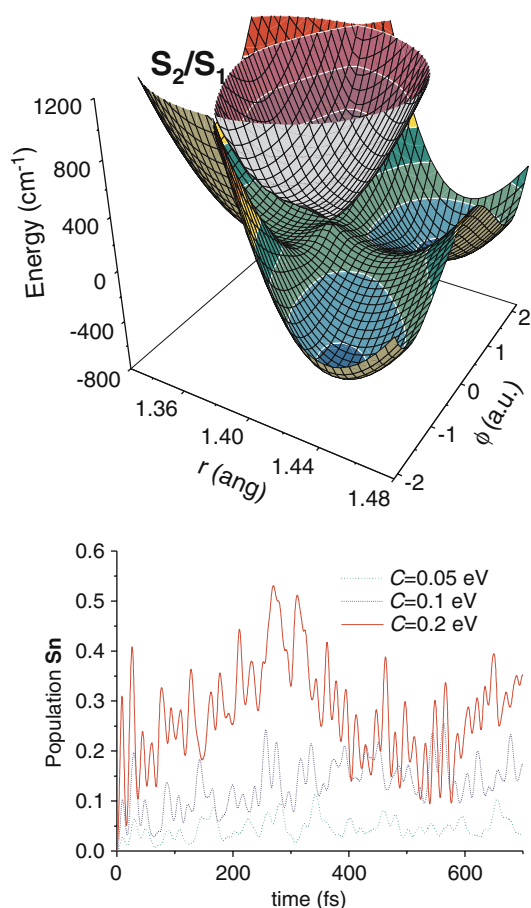


Fig. 6 2D plot of the conical intersection among the S_1 and S_2 excited states in the 2D model of 5f-uracil for the case $C = 0.05$ eV in Eq.8. Time evolution of the population of the S_n state

of the excited state properties of large molecules in solution, reporting some examples of its application to the study of processes of technological or biological interest. Our reference methods for electronic calculations are PBE0 and TD-PBE0, while bulk solvent effect is included by the PCM. On the other hand, it is important to highlight that this can be often considered only the starting and explorative approach: when dealing with complex phenomena like those involving excited states in reactive processes in solution it is important to adopt a flexible strategy, each time selecting the most suitable approach to the process under examination.

It is possible to highlight other general features of our theoretical approach:

1. Tackling molecules as similar as possible to those examined by the experimentalists, limiting the use of simplified models. Although theoretical studies on small model systems have allowed a fundamental advance in the knowledge of the basic mecha-

nisms and processes involved in the excited-state reactivity, it is very important to understand how these basic mechanisms and processes apply in relatively large molecules, as often happens for the molecules of technological and biological interests.

2. Analogously, studying the processes in the condition as similar as possible to that experienced during experiments. In this respect, it is important to be able to treat systems in the condensed phase rather than in the gas phase. Only integrating experimental and computational results it is possible to fully understand complex phenomena; it is thus important to bridge the gap between the molecules/processes studied *in silico* and those examined *in vitro* or *in vivo*.
3. If possible, examining the behavior of all the electronic states potentially interacting with the excited state of interest and exploring the widest portion of the PES as possible. The dynamics can be dramatically influenced by small couplings between the excited states as well as by the “exact” shape of the PES.
4. Even if keeping in mind that it is not always possible that the same approach is suitable for different processes, always preferring easy and conceptual transferable approaches, limiting the use of “ad hoc parameters” and recipes.
5. Coupling computations with the maximum degree of accuracy attainable with explanations in terms of basic and general chemico-physical effects. The dynamical behavior and final outcome of processes involving excited states depend on the composition of many subtle effects and are extremely sensible to small energy variation (also ≤ 1 kcal): it is thus necessary to get as close as possible to the so-called chemical accuracy. On the other hand, resorting to the conceptually simple but powerful traditional tools of the theoretical chemistry (such as molecular orbitals and population analysis) makes easier to infer general and transferable information on the driving forces of the excited state reactions and on the physical-chemical effects that can influence them.
6. Trying to define reduced dimensionality models, based on accurate electronic calculation, for QD studies. There is an extensive literature of QD studies on model systems with simple potentials (i.e. quadratic), mostly suited for photophysical relaxation processes. Nowadays, the increased reliability of accurate electronic calculations allows to characterize the true potential surfaces leading to excited-state reactions in real molecules, showing unusual features like wide plateaux, long and curved

intersection lines, large amplitude motions, etc. As a consequence there is room and need for extensive QD model investigations on these complex-topology surfaces to enquire their dynamical consequences, and how they are modified by environmental effects. Coupling the information obtainable with this approach to the ones from on-the-fly full-coordinate classical trajectory studies, it is probably at hand to get great progress in understanding ultrafast excited state dynamics of real molecules.

In all the examples reported, we have always tried to conform to the above guidelines and we think that it is now possible to perform dynamical studies on the ground of PES computed in the condensed phase with a high degree of accuracy.

The continuous advance in the computational methods makes also likely that in the near future on-the-fly dynamics based on PCM/TD-DFT calculations will be an interesting alternative.

Notwithstanding all the progress of the QM method, further refinements are obviously in order to treat *ab initio* the large majority of processes occurring within systems as large as proteins or nanotechnology devices. A possible strategy to tackle those cases it is to define first what portion of the whole system has to be treated at the QM level; once a suitable subsystem has been tailored, the effect of the remaining part of the system can be easily included in the models we have presented by using the standard recipes of mixed QM/MM methods.[18–21,103–107] On the balance, all the reported results thus suggest that an accurate time-resolved dynamical description of the excited state processes in systems of technological and biological interest is at hand.

References

1. Laane J, Takahashi H, Bandrauk AD (eds) (1998) Structure and dynamics of electronic excited states. Springer, Berlin Heidelberg New York
2. Klessinger M, Michl J (eds) (1995) Excited states and photochemistry of organic molecules VCH, New York
3. Wang CH (1985) Spectroscopy of condensed media. Academic, New York
4. Fleming GR (1986) Chemical applications of ultrafast spectroscopy. Oxford University, New York
5. Assion A, Baumert T, Bergt M, Brixner T, Kiefer B, Seyfried W, Strehle M, Gerber G (1998) Science 282:919
6. Olivucci M, Sinicropi A (2005) Computational photochemistry In: Olivucci M (ed) Computational photochemistry, vol 16. Elsevier, Amsterdam
7. Dreuw A, Head-Gordon M (2005) Chem Rev 105:4009
8. Andersson K, Roos BO (1995) In: Yarkony (ed) Modern electronic structure theory, vol 1. World Scientific, New York, p 55
9. Lami A, Villani G, Theor Chem Acc (this issue)
10. Miller WH (2001) J Phys Chem A 105:2942
11. Beck H, Jäckle A, Worth GA, Meyer H-D (2000) Phys Rep 324:1
12. Granucci G, Persico M, Toniolo A (2001) J Chem Phys 114:10608
13. Olivucci M, Lami A, Santoro F (2005) Angew Chem 44:5118
14. Berger R, Fischer C, Klessinger M (1998) J Phys Chem A 102:7157
15. Grimme S (2004) Rev Comp Chem 20:153
16. Rodriguez-Garcia V, Yagi K, Hirao K, Iwata S, Hirata S (2006) J Chem Phys 125:014109
17. Burke K, Werschnik J, Gross EKV (2005) J Chem Phys 123:62206
18. Wanko M, Hoffmann M, Strodel P, Koslowski A, Thiel W, Neese F, Frauenheim T, Elstner M (2005) J Phys Chem B 109:3606
19. Andruniow T, Ferré N, Olivucci M (2004) Proc Nat Acad Sci 101:17908
20. Sinicropi A, Andruniow T, Ferré N, Basosi R, Olivucci M (2005) J Am Chem Soc 127:11534
21. Toniolo A, Olsen S, Manohar L, Martinez TJ (2004) Faraday Discuss 127:149
22. Bauernshmitt R, Ahlrichs R (1996) Chem Phys Lett 256:454
23. Casida ME, Jamorski C, Casida KC, Salahub DR (1998) J Chem Phys 108:4439
24. Stratmann RE, Scuseria GE, Frisch MJ (1998) J Chem Phys 109:8218
25. Adamo C, Scuseria G, Barone V (1999) J Chem Phys 111:2889
26. Guillemoles JF, Barone V, Joubert L, Adamo C (2002) J Phys Chem A 105:11354
27. Improta R, Barone V (2004) J Am Chem Soc 126:14320
28. Improta R, Santoro F, Diel C, Papastathopoulos E, Gerber G (2004) Chem Phys Lett 387:509
29. Sanna N, Chillemi G, Grand A, Castelli S, Desideri A, Barone V (2005) J Am Chem Soc 127:15429
30. Dierksen M, Grimme S (2005) J Chem Phys 122:244101
31. Van Caillie C, Amos RD (1999) Chem Phys Lett 308:249
32. Van Caillie C, Amos RD (2000) Chem Phys Lett 317:159
33. Furche F, Ahlrichs R (2004) J Chem Phys 117:7433
34. Scalmani G, Frisch MJ, Mennucci B, Tomasi J, Cammi R, Barone V (2006) J Chem Phys 124:094107
35. Wanko M, Garavelli M, Bernardi F, Niehaus TA, Frauenheim T, Elstner M. (2004) J Chem Phys 120:1674
36. Tozer DJ, Amos RD, Handy NC, Roos BO, Serrano-Andres L (1999) Mol Phys 97:859
37. Dreuw A, Weisman JL, Head-Gordon M (2003) J Chem Phys 119:2943
38. Dreuw A, Head-Gordon M (2004) J Am Chem Soc 126:4007
39. Burke K, Werschnik J, Gross EKV (2005) J Chem Phys 123:62206
40. Gritsenko O, Baerends EJ (2004) J Chem Phys 121:655
41. Tawada Y, Tsuneda T, Yanagisawa S, Yanai T, Hirao K (2004) J Chem Phys 120:8425
42. Maitra NT, Zhang F, Cave RJ, Burke K (2004) J Chem Phys 120:5932
43. Maitra NT (2005) J Chem Phys 122:234104
44. Carlotto S, Ferrante C, Maggini M, Polimeno A, Barone V, Benzi C (submitted)
45. Adamo C, Barone V (1999) J Chem Phys 110:6158
46. Bulliard C, Allan M, Wirtz G, Haselbach E, Zachariasse KA (1999) J Phys Chem A 103:7766

47. Rappoport D, Furche F (2004) *J Am Chem Soc* 126:1277
48. Mennucci B, Toniolo A, Tomasi J (2000) *J Am Chem Soc* 122:10621
49. Serrano-Andrés L, Merchán M, Roos BO, Lindh R (1995) *J Am Chem Soc* 117:3198
50. Parusel ABJ, Köhler G, Nooijen M (1999) *J Phys Chem A* 103:4056
51. Levy M, Perdew JP (1993) *Phys Rev B* 48:11638
52. Lieb EH, Oxford S (1981) *Int J Quantum Chem* 19:427
53. Adamo C, Barone V (1998) *Chem Phys Lett* 298:113
54. Improta R, Benzi C, Barone V (2001) *J Am Chem Soc* 123:12568
55. Improta R, Mele F, Crescenzi O, Benzi C, Barone V (2002) *J Am Chem Soc* 124:7857
56. Langella E, Improta R, Barone V (2002) *J Am Chem Soc* 124:11531
57. Zhao Y, Truhlar DG (2005) *J Chem Theory Comput* 1:415
58. Miertus S, Scrocco E, Tomasi J (1981) *Chem Phys* 55:117
59. Tomasi J, Mennucci B, Cammi R (2005) *Chem Rev* 105:2999
60. Cossi M, Barone V (2001) *J Chem Phys* 115:4708
61. Improta R, Barone V, Scalmani G, Frisch MJ (2006) *J Chem Phys* 125:54103
62. Cossi M, Barone V (2000) *J Phys Chem A* 104:10614
63. Aguilar M A (2001) *J Phys Chem A* 105:10393
64. Caricato M, Ingrosso F, Mennucci B, Tomasi J (2005) *J Chem Phys* 122:154501
65. Caricato M, Mennucci B, Tomasi J, Ingrosso F, Cammi R, Corni S, Scalmani G (2006) *J Chem Phys* 124:124520
66. Improta R, Barone V (2004) *J Am Chem Soc* 126:14320
67. Gustavsson T, Banyasz A, Lazzarotto E, Markovitsi D, Scalmani G, Frisch MJ, Barone V, Improta R (2006) *J Am Chem Soc* 128:607
68. Lami A, Petrongolo C, Santoro F (2004) In: Domcke W, Yarkony DR, Koppel H (eds) *Conical intersections, electronic structure, dynamics and spectroscopy*. World Scientific, Singapore
69. Cossi M, Barone V (1999) *J Chem Phys* 109:6246
70. Sharp TE, Rosenstock HM (1964) *J Chem Phys* 41:3453
71. Improta R, Barone V, Santoro F (2006) *Angew Chemie Int Ed* (in press)
72. Santoro F, Improta R, Lami A, Bloino J, Barone V (2006) *J Chem Phys* (submitted)
73. Frisch MJ et al (2005) G03 development version, C02, Gaussian Inc. USA
74. Kosloff R (1996) In: Wyatt RE, Zhang JZH (eds) *Dynamics of molecules and chemical reactions*. Marcel Dekker, New York
75. Lanczos C (1950) *Res Nat Bur Stand* 45:225
76. Ferretti A, Granucci G, Lami A, Persico M, Villani G (1996) *J Chem Phys* 104:5517
77. Merchán M, Serrano-Andres L (2003) *J Am Chem Soc* 125:8108
78. Ismail N, Blancafort L, Olivucci M, Kohler B, Robb MA (2002) *J Am Chem Soc (Commun)* 124:6818
79. Crespo-Hernandez CE, Cohen B, Hare PM, Kohler B (2004) *Chem Rev* 104:1977
80. Blancafort L (2006) *J Am Chem Soc* 128:210
81. Perun S, Sobolewski AL, Domcke W (2005) *J Am Chem Soc* 127:6257
82. Matsika S (2004) *J Phys Chem A* 108:7584
83. Gustavsson T, Sarkar N, Lazzarotto E, Markovitsi D, Barone V, Improta R (2006) *J Phys Chem B* 110:12843
84. Santoro F, Barone V, Gustavsson T, Improta R (2006) *J Am Chem Soc* 128:16312
85. Improta R, Santoro F (2005) *J Phys Chem A* 109:10058
86. Gagliardi L, Orlandi G, Molina V, Malmqvist PA, Roos B (2002) *J Phys Chem A* 106:7355
87. Hohlneicher G, Wrzal R, Lenoir D, Frank R (1999) *J Phys Chem A* 103:8969
88. Improta R, Santoro F (2005) *J Chem Theor Comp* 1:215
89. Vogt G, Nuernberger P, Gerber G, Improta R, Santoro F (2006) *J Chem Phys* 125:044513
90. Nuernberger P, Vogt G, Gerber G, Improta R, Santoro F (2006) *J Chem Phys* 125:044512
91. Marcus RA (1956) *J Chem Phys* 24:4966
92. Marcus RA (1982) *Faraday Discuss Chem Soc* 74:7
93. Marcus RA, Sutin N (1985) *Biochim Biophys Acta* 811:265
94. Cave RJ, Newton MD (1996) *Chem Phys Lett* 249:15
95. Fernandez E, Blancafort L, Olivucci M, Robb MA (2000) *J Am Chem Soc* 122:7528
96. Jolibois F, Bearpark MJ, Klein S, Olivucci M, Robb MA (2000) *J Am Chem Soc* 122:5801
97. Blancafort L, Jolibois F, Olivucci M, Robb MA (2001) *J Am Chem Soc* 123:722
98. Sinicropi A, Pischel U, Basosi R, Nau WM, Olivucci M (2000) *Angew Chemie Int Ed* 39:4582
99. Barone V, Newton MD, Improta R (2006) *J Phys Chem B* 110:12632
100. Improta R, Barone V, Newton MD (2006) *Chem Phys Chem* 7:1211
101. Fantacci S, Migani A, Olivucci M (2004) *J Phys Chem A* 108:1208
102. Rohetgi-Mukherjee KR (1978) *Fundamentals of photochemistry*. Wiley Eastern Edited, New Delhi
103. Hoffmann M, Wanko M, Strodel P, König PH, Frauenheim T, Schulten K, Thiel W, Tajkhorshid E, Elstner M (2006) *J Am Chem Soc* 128:10808
104. Grozema FC, Swart M, Zijlstra RWJ, Piet JJ, Siebbeles LDA, van Duijnen PT (2005) *J Am Chem Soc* 127:11019
105. Groenhof G, Bouxin-Cademartory M, Hess B, de Visser SP, Berendsen HJC, Olivucci M, Mark, AE, Robb MA (2004) *J Am Chem Soc* 126:4228
106. Vreven T, Byun KS, Komaromi I, Dapprich S, Montgomery JA Jr, Morokuma K, Frisch MJ (2006) *J Chem Theory and Comput* 2:815
107. Miyahara T, Tokita Y, Nakatsuji H (2001) *J Phys Chem B* 105:7341